Patterning of FePt for magnetic recording

G.J. Li [a], C.W. Leung [b], Z.Q. Lei [a], K.W. Lin [c], P.T. Lai [a], Philip W.T. Pong [a,*]

[a] *Department of Electrical and Electronic Engineering, The University of Hong Kong, Hong Kong*
[b] *Department of Applied Physics, The Hong Kong Polytechnic University, Hong Kong*
[c] *Department of Materials Science and Engineering, National Chung Hsing University, Taiwan*

ARTICLE INFO

ABSTRACT

Higher areal density for magnetic recording is needed to provide larger storage capacities on harddisk drives. However, as the recording bit size of traditional magnetic recording materials (such as Co/Cr) approaches 10 nm, the magnetic direction of each recording bit would become unstable at room temperature due to thermal fluctuation. To solve this problem, efforts have been made using two methods: one method is to replace the disk media with new materials possessing higher magnetic anisotropy which would lead to better thermal stability; and the second one is to employ different configurations for the recording layer. FePt with patterned media configuration is a combination of these two methods. In this paper we review some novel and interesting methods of patterning FePt for magnetic recording, including thermal patterning, self-assembly patterning, and lithography patterning.

© 2011 Elsevier B.V. All rights reserved.

1. Introduction

Higher areal density is needed in magnetic recording to provide more storage capacity on a harddisk drive. However, when the recording bit is down to 10 nm scale, the recording bit might flip itself due to thermal fluctuation and renders the recording data unstable. There are two methods to acquire higher areal density: one is to acquire materials with larger magnetic anisotropy; the other one is to fabricate patterned media with space among each bit.

Iron platinum is a binary alloy and stoichiometric FePt has two different crystal structures: face center cubic (fcc) phase and face center tetragonal (fct) phase (Fig. 1). Fcc phase FePt has a c/a ratio of 1 while fct phase has c/a ratio of 0.968 [1]. The fcc phase FePt behaves as superparamagnetic at sub 10 nm scale while fct FePt still behaves as ferromagnetic because of its huge magnetic anisotropy due to the strong coupling of 3 d and 5 d electrons [2]. FePt nanoparticles can be synthesized by chemical processes [3], sputtering [4], and even gas condensation methods [5]. However, method for direct synthesis of pure fct phase FePt is not yet reported. After FePt nanoparticles or thin films are synthesized, inert gas protective annealing is needed to transform fcc phase FePt to fct phase FePt [6]. It is reported that 580 °C was needed to fully transform the fcc phase to fct phase without additional catalyst [7].

Patterned media recording [8] was proposed to enhance the thermal stability by inserting space among each recording bit. With this arrangement, the grains in the same bit strongly couple with each other. As a result, the whole bit behaves as a single domain. Thus the volume of each domain increases and the thermal stability is enhanced. There are a number of nanoscale fabrication methods which are capable of fabricating patterned media at nanoscale. However, an efficient and economical method is needed for industrial application. Since FePt material has sufficient thermal stability at nanoscale, patterned media recording together with FePt is a promising choice for ultimate ultrahigh density magnetic recording.

For patterning FePt, a number of methods have been investigated. These patterning methods are categorized in Table 1 according to the nature of each patterning method. In this article, we discuss the patterning methods of FePt including thermal patterning [9,10], self-assembly patterning of FePt nanoparticles [11–13], and lithography patterning of FePt thin film [14–21] and their challenges for industrial application.

2. Patterning of FePt

FePt possesses the following properties: fct phase FePt can be transformed from fcc phase through annealing [6,22]; FePt can exist as ferromagnetic nanoparticles at sub 10 nm size; FePt can also be sputtered as thin film. These properties are all utilized to fabricate FePt patterned media. In the following parts, we discuss the different patterning methods of FePt including thermal patterning, self-assembly patterning, and lithography patterning.

2.1. Thermal patterning

Heating effects of laser can be used to pattern FePt at nanoscale. Fct phase FePt and fcc phase FePt can be transformed into each other

---

* Corresponding author.
E-mail address: ppong@eee.hku.hk (P.W.T. Pong).

Fe atom
Pt atom

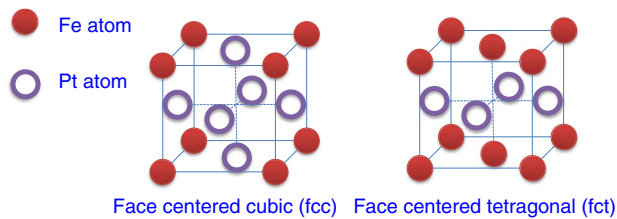Face centered cubic (fcc) Face centered tetragonal (fct)

Fig. 1. Crystal structures of fcc and fct phase FePt.

Fig. 2. Enthalpy-temperature picture of FePt. T_g is the glass transition temperature and T_m is the melting temperature of FePt.

through different cooling strategies like other phase change materials such as $Ge_2Sb_2Te_5$ [23,24]. The disordering process, which is the phase transformation from fct phase to fcc phase, can be described by A–B–C–D–E–F processes in the temperature enthalpy picture in Fig. 2. In A–B process, the fct phase FePt is heated and the system thermal enthalpy increases as the temperature increases. In B–C process, the heating of fct phase FePt continues and melting process is going on, thus the thermal enthalpy increases. In C–D process, the melted FePt is being heated and the temperature is still increasing. For D–E process, the heating stops suddenly and results in the rapid dropping of the FePt temperature. This process can be regarded as a supercooling process. After dropping below the melting temperature and the further cooling process of E–F, FePt solidates and becomes fcc phase FePt. Meanwhile, the ordering process of phase transformation from fcc phase to fct phase FePt can be initiated by two different methods. One is heating FePt over the melting point (F–E–D–C–B–A) and the other one is by heating FePt to the glass transition temperature (F–G–H–A). The glass-to-crystalline process does not require heating up to the melting point, and this method for annealing FePt has been frequently investigated [25–28]. In F–G process, fcc phase FePt is heated over the glass transition temperature. Then in G–H process, the FePt is cooling with a rather slow speed, and FePt starts to transform from fcc phase to fct phase. The H–A process also needs a rather slow cooling speed to form good quality thin film. It is found that annealing at 580 °C for 30 min is enough to transform fcc phase FePt to fct phase FePt [29]. So the glass transition temperature for FePt is not larger than 580 °C. Since laser is a very localized and effective means for heating, transformations between fcc phase FePt and fct phase FePt can be achieved by laser with different pulse widths.

The fcc phase to fct phase transformation was investigated by Hamann et al., using a 532 nm laser with pulse width of 10 second and the absorbed laser power of 4 mW [10]. Since the pulse width is rather long, the illuminating process can be regarded as a slow cooling process and thus the fcc phase FePt will be transformed to fct phase. A fcc phase FePt thin film was first chemically synthesized and dispersed on Si/SiO₂ substrate. Then the sample was heated by the 532 nm laser. Patterns over large area can be illuminated by scanning the sample over the x- and y- directions. The heating temperature was estimated to be around 550 °C which is lower than the FePt melting temperature, so the process can be identified as a glass to crystalline
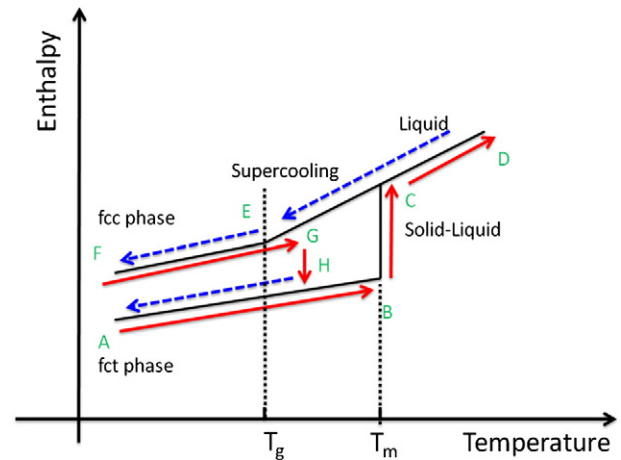
transformation process. As a result, micro-sized patterns of fct phase FePt were acquired on the fcc phase FePt thin film. Dots of diameter as small as 3 μm were fabricated using this setup.

The fct phase to fcc phase transformation was also investigated using 25 ns pulses of 248 nm KrF laser with pulse frequency of 10 Hz and pulse power ranging from 0.05 to 2.0 J/cm² [9]. Since the pulse width was quite short, the annealing process can be regarded as a supercooling process. The FePt thin film here was epitaxially grown on an MgO substrate in high vacuum by pulsed laser deposition (PLD). The sample was heated during deposition so most of the deposited FePt was fct phase although there may still be some fcc phase FePt. After annealing, the laser spot was focused perpendicularly onto the substrate. The sample was moved forward step by step, so a line pattern was formed on the sample. The number of pulses for patterning each bit is adjustable, so the heat absorbed by the sample during this process can be adjusted. If the number of laser pulses is small, the fct phase FePt will first melt and then undergo supercooling and finally turn into fcc phase FePt. If the number of laser pulses is large, the induced heat can be seen as a continuous annealing process and FePt will remain in the fct phase. If the number of laser pulse is large enough, the coercivity might even increase due to the transformation of the remaining fcc phase FePt in the as-deposited state into fully fct phase FePt. Fig. 3(a) shows that when the number of laser pulses increases, the intensities of fct phase characteristic peaks (001) and (200) also increase. This indicates that there is more fct phase FePt formation than the as-deposited state. The patterned structures after annealing are shown in Fig. 3(b). Dots with a minimum diameter of 10 μm were achieved on the fcc phase FePt.

Fabrication of patterned recording media with laser annealing FePt thin film is a novel method. Different phases of FePt can be transferred into each other by controlling the number of laser pulses. Since laser

Table 1
Methods of patterning FePt for magnetic recording. Nil: not reported. (Nil: not reported).

Category	Method	Bit size	Annealing temperature (°C)	XRD characteristic peak	Coercivity (kOe)	Reference
Laser patterning	PLD annealing	1 μm	300–900	(001)	3	[9]
	Laser annealing	800 nm	580	Nil	Nil	[10]
Self-assembly	On SiO₂	3.2 nm	650	(110)	0	[11]
	On glass	50 nm	700	(001)	20	[12]
	On patterned media	5 μm	800	(111)	1	[13]
Lithography	EBL	1 μm	800	Nil	9.5	[14]
	Nearfield lithography	250 nm	Nil	Nil	Nil	[15]
	UV lithography	2 μm	700	Nil	12.4	[16]
	UV + Sputter/PLD	200 nm	700	(001)(110)	15	[17]
	Nanosphere	200 nm	550	Nil	2.5	[18]
	Self-assembly template	100 nm	245	Nil	Nil	[19]
	Template + sputter	5 nm	600	Nil	8.3	[20]
	Langmuir-Blodgett film	1 μm	Nil	(111)(220)	Nil	[21]
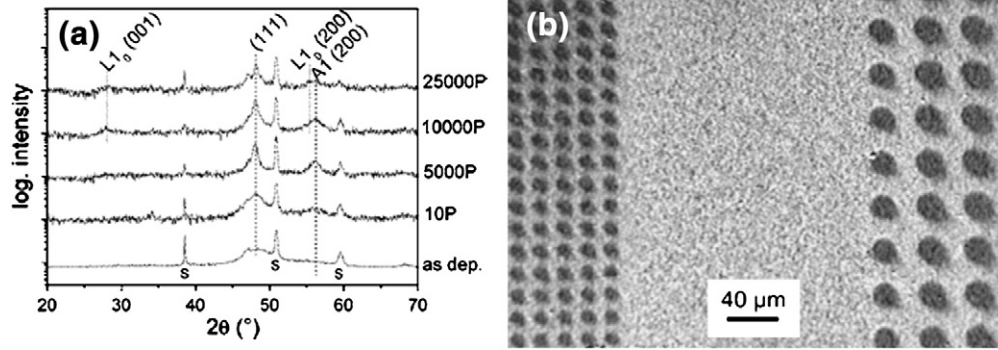
Fig. 3. XRD and SEM image of laser annealing patterned FePt. (a) the XRD analysis of annealed FePt with different laser pulses [9]. As the number of laser pulses increases, the intensities of specialized peaks such as (001) and (200) peaks increase, indicating more fct phase FePt formation in the samples. (b) the Kerr microscopy image of patterned FePt [9]. The dark dots are fct phase FePt while the background are the fcc phase FePt. Reprinted with permission from [9].

patterning of FePt makes use of phase transformation and does not change the FePt volume, the patterned surface can be made very smooth using this method. In nowadays harddisk drive recording technology, the distance between the recording head and the recording media is only approximately 1 nm. Thus even a small roughness of recording media would damage the recording head. So the advantage of generating smooth surfaces by using laser patterning of FePt is obvious. However, there are still some problems to solve before this method can be adopted for industrial-scale production. For example: solid immersion lenses [30,31] or other methods [32,33] are needed to focus the laser beam into a sub-wavelength scale in order to acquire nanoscale patterns; high speed moving stage [34] might be needed for industrial application; the cost for laser patterning is rather low compared to electron beam lithography but the time needed for laser annealing is still too long.
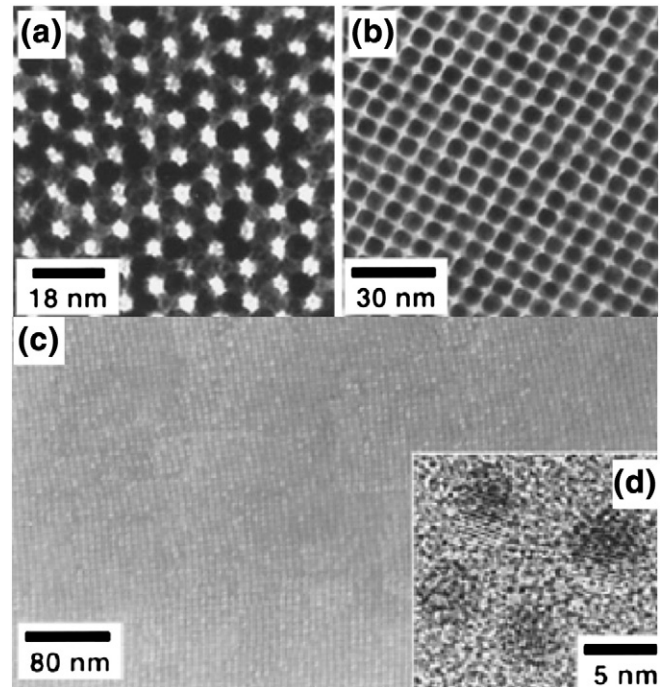
2.2. Self-assembly patterning

Self-assembly patterning is a process for patterning components within a short distance spontaneously without any external force. The self-assembly patterning process can be comparable with crystallization, where elements rearrange themselves into a crystal structure [35]. However, different from the strong chemical interactions in crystal structures, the forces driving nanoparticles to self-assemble are weak hydrogen bond, van der Waals force, and electric/magnetic dipole interaction force.

Direct self-assembly patterning of FePt was first proposed by Sun et al. [3] in 2000. Platinum acetylacetonate and iron pentacarbonyl served as Pt and Fe sources respectively. $Pt(acac)_2$ and $Fe(CO)_5$ decompose in high temperature and as a result FePt can be synthesized. In this method, the composition of the FePt can be controlled by adjusting the ratio of iron carbonyl to platinum salt. The size of the FePt nanoparticles can also be tuned by the thickness of the seed layer. The synthesized FePt nanoparticles can be dispersed in many kinds of solvents and thus they can be patterned by self-assembly. This method has been repeated many times [13,36] because it is an effective and quick method for fabricating fct FePt patterns with good thermal stability. Further improvement such as the rapid thermal annealing [6,37,38] and salt matrix addition [39,40] were investigated to prevent FePt sintering, and FePt nanoparticles were patterned with well order in about 500 nm scale. The patterned and annealed results of self-assembly patterning [3] are given in Fig. 4. From Fig. 4(a)(b)(c), we can see that the FePt nanoparticles can be patterned with well order in about 500 nm scale. The annealed FePt nanoparticles image in Fig. 4(d) also indicates that after annealing the patterns are still well preserved.

FePt patterning using self-assembly is a very effective method for patterning FePt at short range. For further application, we need to overcome the challenges of precisely controlling the patterning order over a few hundred microns and expediting the fabrication process.

2.3. Lithography

Lithography is a top–down fabrication technique widely used in industry and research, and it can also be used for patterning FePt thin film in magnetic recording. Lithography can be divided into two groups depending on whether mask is used or not. Maskless lithography includes electron beam lithography (EBL), focused ion beam lithography (FIB), and laser machining lithography [41]. Templated lithography includes UV lithography, nanoimprint lithography, and nanosphere lithography. Among these technologies, EBL [42,43], FIB [44], UV lithography [17], nanoimprint [45] and nanosphere lithography [18] were investigated to pattern FePt for magnetic recording. Fig. 5 shows some patterns fabricated by EBL with different sizes. The patterns are of good quality with sharp edges and only a few defects. Nanosphere lithography is capable of growing nanoscale patterns over a large area. The nanospheres used in this method are self-assembly patterned on the sample surface and serve as an etching template. Using different sizes of nanospheres, different

Fig. 4. TEM images of patterned FePt monolayer by direct self-assembly [3]. (a) TEM image of 6 nm FePt nanoparticles on SiO coated copper grid from hexane acid. (b) TEM image of 6 nm FePt nanoparticles on SiO copper grid from hexanoic acid. (c) High resolution TEM of 4 nm FePt after annealing. (d) HRTEM of 4 nm FePt on SiO coated copper grid after annealing. Reprinted with permission from [3].
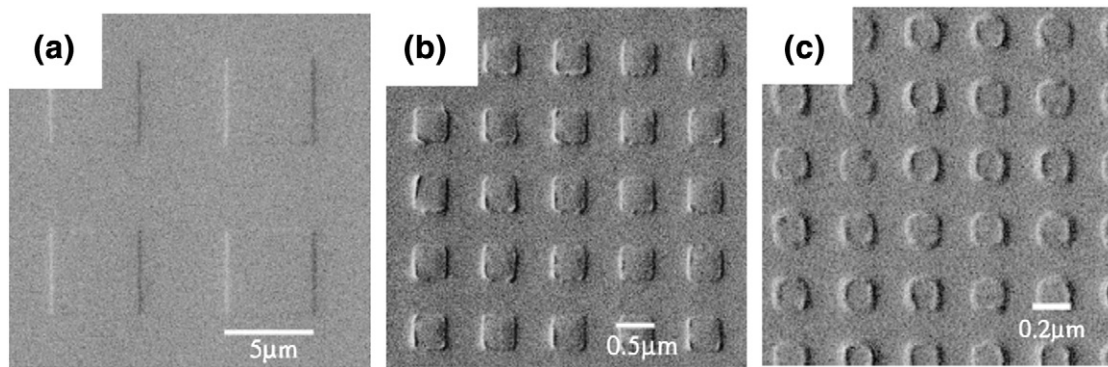
Fig. 5. SEM images of patterned FePt using EBL [43]. The sizes of each patterns are (a) 5 μm × 5 μm, (b) 500 nm × 500 nm, and (c) 200 nm × 200 nm. Reprinted with permission from [43].
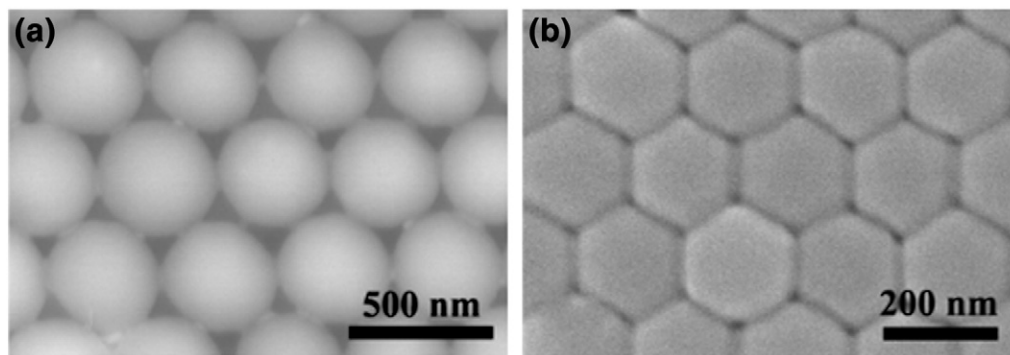

Fig. 6. SEM image of self-assembled nanospheres [46]. (a) 440 nm diameter nanospheres. (b) 200 nm diameter nanospheres. Reprinted with permission from [46].

periodic templates can be fabricated. Nanosphere lithography patterning of FePt was carried out using 200 nm nanospheres in [18]. The template was fabricated through self-assembled polystyrene nanospheres with mean size of 200 nm (Fig. 6(a)) and 440 nm (Fig. 6(b)) respectively [46]. Then FePt is deposited on SiO_2 substrate through the nanospheres template. After that, the nanospheres template is removed by rinsing in acetone. Fig. 7(a) shows the AFM image of the patterned FePt. The shape of the pattern is a triangular prism which is a negative of the mask. Fig. 7(b) gives the height distribution of FePt patterns and height is ranging from 26 nm to 36 nm. However, this height variation is beyond the tolerance of nowadays harddisk drive media. Besides, nanospheres lithography suffers the problems of incomplete removal of spherical templates [47], difficulty in recycling the templates [48,49], and imperfection over long range [50]. Thus these inherent problems of nanospheres lithography need to be solved before industrial application for patterning FePt.

Maskless lithography offers good resolution but involves high cost. Templated lithography is of low cost but its resolution in general is not as good. Nanosphere lithography may offer an alternative for high resolution lithography; however, some inherent problems are still challenges for industrial application.

3. Conclusion

Different methods for patterning FePt are discussed in this article. A model for FePt thermal phase transformation principle is given. Thermal patterning of FePt provides a smooth surface which is crucially important for magnetic recording. Self-assembly patterning of FePt can provide high areal density; however, it is not easy to reproducibly pattern FePt with long-range order by self-assembly. Maskless lithography involves high cost and its throughput is not high enough for industry. Templated lithography patterning is of low cost and high throughout but its resolution in general is not as good. Nanosphere
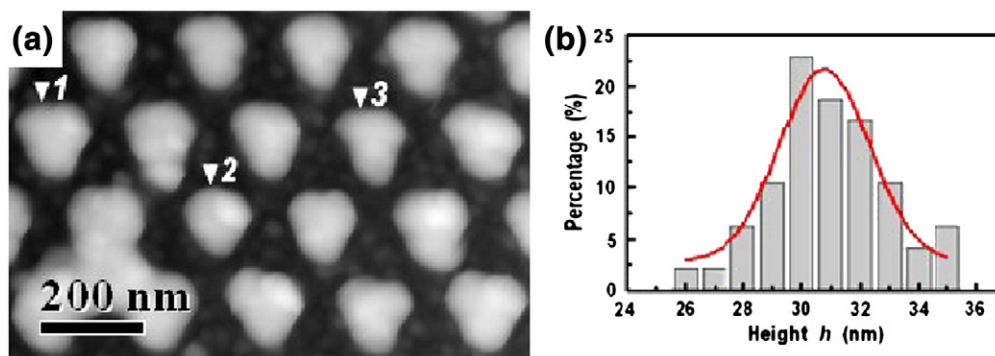

Fig. 7. AFM images of nanospheres patterned FePt [18]. (a) AFM image of patterned FePt. (b) Height distribution of FePt patterns. Reprinted with permission from [18].

lithography offers higher resolution but further investigations are needed for overcoming some technical challenges.

Acknowledgment

References

[1] S.V. Halilov, R. Feder, Solid State Commun 88 (10) (1993) 749.
[2] A.B. Shick, O.N. Mryasov, Phys. Rev. B 67 (17) (2003) 172407.
[3] S.H. Sun, C.B. Murray, D. Weller, L. Folks, A. Moser, Science 287 (5460) (2000) 1989.
[4] A. Breitling, D. Goll, J. Magn. Magn. Mater. 320 (8) (2008) 1449.
[5] S. Stappert, B. Rellinghaus, M. Acet, E.F. Wassermann, J. Cryst. Growth 252 (1–3) (2003) 440.
[6] H. Zeng, S.H. Sun, R.L. Sandstrom, C.B. Murray, J. Magn. Magn. Mater. 266 (1–2) (2003) 227.
[7] T.S. Vedantam, J.P. Liu, H. Zeng, S. Sun, J. Appl. Phys. 93 (10) (2003) 7184.
[8] R.L. White, R.M.H. New, R.F.W. Pease, IEEE Trans. Magn. 33 (1) (1997) 990.
[9] J. Buschbeck, S. Fahler, M. Weisheit, K. Leistner, J. McCord, B. Rellinghaus, L. Schultz, J. Appl. Phys. 100 (12) (2006) 123901.
[10] H.F. Hamann, S.I. Woods, S.H. Sun, Nano Lett. 3 (12) (2003) 1643.
[11] J.-G.Z.M. Tanase, C. Liu, N. Shukla, T.J. Klemmer, D. Weller, D.E. Laughlin, Metall. Mater. Trans. A/4 (2007) 798.
[12] G.P. Lin, P.C. Kuo, K.T. Huang, C.L. Shen, T.L. Tsai, Y.H. Lin, M.S. Wu, Thin Solid Films 518 (8) (2010) 2167.
[13] O. Yildirim, T. Gang, S. Kinge, D.N. Reinhoudt, D.H.A. Blank, W.G. van der Wiel, G. Rijnders, J. Huskens, Int. J. Mol. Sci. 11 (3) (2010) 1162.
[14] A. Breitling, T. Bublat, D. Goll, Physica 3 (5) (2009) 130.
[15] C.H. Chang, C.W. Tan, J.M. Miao, G. Barbastathis, Nanotechnology 20 (49) (2009) 495301.
[16] M. Chen, D.E. Nikles, H.Q. Yin, S.T. Wang, J.W. Harrell, S.A. Majetich, J. Magn. Magn. Mater. 266 (1–2) (2003) 8.
[17] L.J. Qiu, J. Ding, A.O. Adeyeye, J.H. Yin, J.S. Chen, S. Goolaup, N. Singh, IEEE Trans. Magn. 43 (6) (2007) 2157.
[18] H. Zhong, G. Tarrach, P. Wu, A. Drechsler, D. Wei, J. Yuan, Nanotechnology 19 (9) (2008) 095703.
[19] S.B. Darling, N.A. Yufa, A.L. Cisse, S.D. Bader, S.J. Sibener, Adv. Mater. 17 (20) (2005) 2446.
[20] Y.J. Tang, J.F. AuBuchon, L.H. Chen, S. Jin, J.W. Kim, Y.H. Kim, C.S. Yoon, J. Appl. Phys. 99 (8) (2006) 08G909.
[21] Q.J. Guo, X.W. Teng, H. Yang, Adv. Mater. 16 (15) (2004) 1337.
[22] F.E. Spada, F.T. Parker, C.L. Platt, J.K. Howard, J. Appl. Phys. 94 (8) (2003) 5123.
[23] T.S. Kao, Y.H. Fu, H.W. Hsu, D.P. Tsai, J. Microsc-Oxford 229 (3) (2008) 561.
[24] Y.H. Fu, Y.L. Lu, P.H. Chang, W.C. Hsu, S.Y. Tsai, D.P. Tsai, Jpn. J. Appl. Phys. 45 (9A) (2006) 7224 1.
[25] S. Saita, S. Maenosono, J. Phys. Condens. Mat. 16 (36) (2004) 6385.
[26] C. Liu, X.W. Wu, T. Klemmer, N. Shukla, D. Weller, Chem. Mater. 17 (3) (2005) 620.
[27] B. Yao, R.V. Petrova, R.R. Vanfleet, K.R. Coffey, J. Appl. Phys. 99 (8) (2006) 08E913.
[28] S. Momose, H. Kodama, W. Yamagishi, T. Uzumaki, Jpn. J. Appl. Phys. 46 (45-49) (2007) L1105 2.
[29] M.H. Lu, T. Song, T.J. Zhou, J.P. Wang, S.N. Piramanayagam, W.W. Ma, H. Gong, J. Appl. Phys. 95 (11) (2004) 6735.
[30] E. Ramsay, N. Pleynet, D. Xiao, R.J. Warburton, D.T. Reid, Opt. Lett. 30 (1) (2005) 26.
[31] D.R. Mason, M.V. Jouravlev, K.S. Kim, Opt. Lett. 35 (12) (2010) 2007.
[32] X.F. Yang, B.B. Zeng, C.T. Wang, X.G. Luo, Opt. Express 17 (24) (2009) 21560.
[33] V.M. Murukeshan, K.V. Sreekanth, Opt. Lett. 34 (6) (2009) 845.
[34] A. Endo, IEEE J. Sel. Top Quant. 10 (6) (2004) 1298.
[35] S.H. Sun, Adv. Mater. 18 (4) (2006) 393.
[36] C. Verdes, J. Ahner, P.M. Jones, N. Shukla, R.W. Chantrell, D. Weller, Appl. Phys. Lett. 86 (26) (2005).
[37] K. Yano, V. Nandwana, N. Poudyal, C.B. Rong, J.P. Liu, J. Appl. Phys. 104 (1) (2008) 013918.
[38] L.Y. Lu, D. Wang, X.G. Xu, Y. Zhan, Y. Jiang, J. Phys. Chem. C 113 (46) (2009) 19867.
[39] D.R. Li, N. Poudyal, V. Nandwana, Z.Q. Jin, K. Elkins, J.P. Liu, J. Appl. Phys. 99 (8) (2006) 08E911.
[40] C.B. Rong, N. Poudyal, G.S. Chaubey, V. Nandwana, Y. Liu, Y.Q. Wu, M.J. Kramer, M.E. Kozlov, R.H. Baughman, J.P. Liu, J. Appl. Phys. 103 (7) (2008) 07E131.
[41] Z. Kantor, Thin Solid Films 453–54 (2004) 350.
[42] K. Liu, C.L. Ho, S. Aouba, Y.Q. Zhao, Z.H. Lu, S. Petrov, N. Coombs, P. Dube, H.E. Ruda, W.Y. Wong, I. Manners, Angew. Chem. Int. Ed. 47 (7) (2008) 1255.
[43] T. Seki, T. Shima, K. Yakushiji, K. Takanashi, G.Q. Li, S. Ishio, J. Appl. Phys. 100 (4) (2006) 043915.
[44] F. Albertini, L. Nasi, F. Casoli, S. Fabbrici, P. Luches, G.C. Gazzadi, A. di Bona, P. Vavassori, S. Valeri, S.F. Contri, J. Appl. Phys. 104 (5) (2008) 053907.
[45] R.N. Patel, A.T. Heitsch, C. Hyun, D.M. Smilgies, A. de Lozanne, Y.L. Loo, B.A. Korgel, Accs. Appl. Mater. Inter. 1 (6) (2009) 1339.
[46] P.W. Wu, L.Q. Peng, X.L. Tuo, X.G. Wang, J. Yuan, Nanotechnology 16 (9) (2005) 1693.
[47] S.W. Kim, S. Kim, W.Y. Lee, T. Hyeon, J. Am. Chem. Soc. 124 (26) (2002) 7642.
[48] Y.J. He, Mater. Res. Bull. 40 (4) (2005) 629.
[49] J.C. Bao, Y.Y. Liang, Z. Xu, L. Si, Adv. Mater. 15 (21) (2003) 1832.
[50] S.M. Weekes, F.Y. Ogrin, W.A. Murray, Langmuir 20 (25) (2004) 11208.